Asian Journal of Chemistry; Vol. 38, No. 6 (2026), 1493-1504
ASIAN JOURNAL OF CHEMISTRY
https://doi.org/10.14233/ajchem.2026.35525

Assessment of Bioactive Compounds from Aerial Part of *Andrographis paniculata* against Bacteria Involved in Urinary Tract Infection and Glucosamine-6-phosphate Synthase (2VF5) of *E. coli*: *in vitro* and *in silico* Study

EKOMOBONG ARCHIMEDES OKPO[1,*], WAFA ALI ELTAYB[2], GODWIN JOHN EGBE[1], AKEEM AYODEJI AGBOKE[3], CHINWEIZU EJIKEME UDOBI[3], INIOBONG EBENGE ANDY[1], MAAWEYA E. AWADALLA[4], REHAM M. ALAHMADI[5], EHSSAN MOGLAD[6], MOHNAD ABDALLA[7,*] and UWEM OKON EDET[8,*]

[1]Department of Microbiology, Faculty of Biological Sciences, University of Calabar, Calabar, Cross River State, Nigeria
[2]Biotechnology Department, Faculty of Science and Technology, Shendi University, Shendi 11111, Nher Anile, Sudan
[3]Department of Pharmaceutical Microbiology and Biotechnology, University of Uyo, Akwa Ibom State, Nigeria
[4]Research Center, King Fahad Medical City, Riyadh, Saudi Arabia
[5]Department of Botany and Microbiology, College of Science, King Saud University, P.O. Box 22452, Riyadh 11495, Saudi Arabia
[6]Department of Pharmaceutics, College of Pharmacy, Prince Sattam bin Abdulaziz University, P.O. Box 173 Alkharj 11942, Saudi Arabia
[7]Pediatric Research Institute, Children's Hospital Affiliated to Shandong University, Jinan, Shandong 250022, P.R. China
[8]Department of Microbiology, School of Pure and Applied Sciences, Federal University of Technology, Ikot Abasi, Akwa Ibom State, Nigeria

*Corresponding authors: E-mail: ekomarchims20@gmail.com; mohnadabdalla200@gmail.com

Received: 27 December 2025 *Accepted*: 25 April 2026 *Published online*: 31 May 2026 AJC-22375

Urinary tract infections (UTIs) are the most common bacterial infections and are frequently caused by pathogens such as *Escherichia coli*, *Klebsiella pneumoniae* and *Proteus mirabilis*. Increasing antibiotic resistance has intensified the search for alternative antibacterial agents. In this study, extracts and bioactive compounds from *Andrographis paniculata* were evaluated against GlcN-6-P synthase, a key enzyme involved in bacterial peptidoglycan biosynthesis. Antibacterial activity was assessed using the agar well diffusion method, while molecular docking, molecular dynamics simulation and ADMET analyses were performed to evaluate binding affinity, stability and drug-likeness. The ethyl acetate fraction exhibited the highest antibacterial activity against multidrug-resistant uropathogens (MIC = 6.25 mg/mL; MBC = 12.5 mg/mL). Among the isolated compounds, PubChem IDs 15172, 1110 and 102916 showed the strongest binding affinities of -5.4, -5.2 and -5.1 kcal/mol, respectively. All ligands satisfied Lipinski's rule of five and demonstrated favourable pharmacokinetic properties without hepatotoxicity. Molecular dynamics simulations identified compound 15172 as the most stable ligand with minimal conformational fluctuations. These findings suggest that the bioactive compounds from *A. paniculata* possess promising antibacterial and drug-like potential for the development of alternative therapies against UTI-associated pathogens.

Keywords: *Andrographis paniculata*, Bioactive compounds, Urinary tract infection, Molecular docking, Pharmacokinetics.

INTRODUCTION

Urinary tract infection (UTI) is an infection affecting any part of the urinary system including the kidneys, ureters, bladder and urethra [1]. UTIs are among the most common infections worldwide [1,2], particularly in women, and are mainly caused by bacterial pathogens, although fungi and viruses may also contribute [3]. Nearly 50% of women experience at least one UTI during their lifetime due to anatomical factors such as a shorter urethra and its close proximity to the anus, which facilitates bacterial entry into the urinary tract [4,5]. In men, the incidence is comparatively lower but increases with age due to the enlargement of prostate and other urinary tract abnormalities [4].

Escherichia coli is the predominant causative agent of UTIs, accounting for approximately 70-95% of community-acquired infections [5,6]. Other important uropathogens include *Klebsiella pneumoniae, Proteus mirabilis* and *Staphylococcus*

saprophyticus. In hospitalised patients and individuals with indwelling catheters, multidrug-resistant organisms such as *Pseudomonas aeruginosa* and *Enterococcus* species are also frequently associated with UTIs [7].

Bacteria have evolved several mechanisms to resist antibiotics commonly used for the treatment of urinary tract infections (UTIs) [3,7]. The increasing prevalence of antibiotic-resistant uropathogens, particularly uropathogenic *Escherichia* coli (UPEC), has become a major global health concern, leading to treatment failure and increased healthcare costs [8,9]. This challenge has intensified the search for alternative antimicrobial agents, especially from medicinal plants known to contain diverse bioactive compounds with therapeutic potential [10]. *Andrographis paniculata*, commonly known as the "King of Bitters," is a medicinal plant belonging to the family Acanthaceae [11]. Native to South and Southeast Asia, it has been widely used in traditional medicine for the treatment of fever, dysentery, malaria and other infectious diseases [12,13]. Several studies have reported significant antibacterial activity of phytochemicals isolated from *A. paniculata* and related medicinal plants against different pathogenic microorganisms [14-18]. In Nigeria, the plant is traditionally known as "Ewe korobi-jogbo" or "Meje Meje" among the Yoruba people due to its intensely bitter taste [19]. Despite its ethnomedicinal importance and documented antimicrobial properties, limited studies have evaluated its activity against UTI-associated pathogens such as *E. coli* [20-22].

Recent advances in computational biology have shown that *in silico* methods such as molecular docking and molecular dynamics simulation are valuable tools for identifying and optimizing potential antimicrobial compounds [14,23]. Therefore, this study integrated both *in vitro* and *in silico* approaches to evaluate the antibacterial activity and drug-like properties of *A. paniculata* bioactive compounds against UTI pathogens. Particular emphasis was placed on glucosamine-6-phosphate synthase (GlmS), an essential bacterial enzyme involved in peptidoglycan biosynthesis and absent in humans, making it a promising target for antimicrobial drug development.

EXPERIMENTAL

Collection and extraction of *Andrographis paniculata* crude extract: The aerial parts of *A. paniculata* (leaves, stems and flowers) were collected from a local garden in Calabar City during the flowering stage in October, 2025. Plant materials were manually harvested, washed with sterile distilled water and dried at low temperature to minimize microbial contamination and preserve bioactive constituents. The dried samples were pulverized using a mortar and pestle and sieved through a 40-60 mm mesh to obtain a finely powder.

The powdered material was divided into two portions and separately macerated in 3 L of distilled water and 3 L of methanol. The aqueous extract was filtered after 24 h, while the methanolic extract was filtered after 72 h using sterile muslin cloth, cotton wool and Whatman No. 1 filter paper. The filtrates were concentrated using a water bath at 40 ºC and further dried in a vacuum desiccator. The crude extracts were weighed, sealed with aluminium foil and stored at 4 ºC until further analysis.

Fractionation of *A. paniculata* extract: The extract of *A. paniculata* was fractionated using vacuum liquid chromategraphy (VLC) with solvent systems of increasing polarity, namely *n*-hexane, dichloromethane, ethyl acetate and methanol. The obtained fractions were concentrated to dryness using a water bath at 40 ºC and weighed to determine percentage yield. Each fraction was screened for antibacterial activity and active fractions were further evaluated for minimum inhibitory concentration (MIC) and minimum bactericidal concentration (MBC) against susceptible microorganisms [24].

Evaluation of the isolated fractions: The *in vitro* antibacterial activity of the different fractions obtained from *A. paniculata* extract was tested using the agar well diffusion method. Dimethylsulfoxide (DMSO) was used to dissolve the fractions. The bacterial suspensions were diluted to a turbidity of approximately 0.5 McFarland ($\approx 1.5 \times 10^8$ CFU/mL). Mueller-Hinton agar (MHA) plates were seeded with the test organisms. A cork borer was used to create walls on the agar. Ciprofloxacin antibiotic was used as a positive control and 50% DMSO was used as a negative control. A micropipette was used to deliver the isolated fractions into the well. The plates were incubated at 37 ºC for 24 h, after which the diameter of the zone of inhibition around each well was measured and recorded. Each experiment was performed in duplicates.

The MIC values were determined for bacteria that were sensitive to the bioactive compound during the agar well diffusion assay. To accomplish this, the bacteria inocula were prepared from a 12 h broth culture and the suspensions were adjusted to a turbidity of 0.5 McFarland. A susceptibility test was conducted using the standard broth microdilution method following the Clinical and Laboratory Standard Institute guidelines on Muller-Hinton broth (MHB) with an inoculum of 5×10^4 CFU/mL. The MHB was then supplemented with serial dilution of the bioactive compound (*i.e.*, different concentrations of the bioactive compound). The lowest concentration of the bioactive compound that was capable of inhibiting visible growth after 24 h of incubation at 37 ºC was recorded as the MIC. To determine the MBC, a dilution representing the MIC and two more concentrated dilutions of the test fraction were plated and counted to determine the survival CFU/mL of the tested multidrug-resistant uropathogens. The lowest concentration that was capable of inhibiting 99.9% of the activity of the tested bacteria was taken as the MBC.

Retrieval and preparation of the ligands and protein: Glucosamine-6-phosphate synthase (GlmS) is a key enzyme involved in peptidoglycan biosynthesis and has emerged as an important molecular target for the development of antimicrobial and antidiabetic agents [25-27]. In present study, the three-dimensional structure of GlmS (PDB ID: 2VF5) was retrieved from the Protein Data Bank based on previously published reports [28]. The ligand molecules used for molecular docking were identified from the GC–MS analysis of *A. paniculata* extracts. The ligands selected for this study and their respective PubChem CIDs were hexanoic acid (8892), ethyl 2-ethylhexanoate (102916), 3-buten-2-ol, 4-phenyl- (15172), 2-(1-ethoxyethoxy)succinic acid, diethyl ester (51328950), butanedioic acid (1110) and undeca-3,4-diene-

2,10-dione (538547). All the selected ligands had their energies minimised for docking as reported previously [29]. The target protein was prepared using the Biovia Studio [30]. Following preparations, the coordinates of the proteins were revealed to be x = 29.2968, y = 18.7548 and Z = -2.1605, respectively. The prepared ligands and proteins were then saved for docking and simulation analyses.

Molecular docking: The prepared ligands and target protein were subjected to molecular docking using the Auto-Vina docking tool version 4.2 following previously reported procedures [29]. The active site of the protein was identified with the aid of the native ligand using the Allosite tool [31]. Subsequently, the ligands were docked individually into the binding pocket employing the London scoring function [32]. The resulting docking poses and protein–ligand interactions were visualized in two and three dimensions using Biovia and PyMOL software, respectively [33].

Molecular dynamics simulation (MDS), principal component analysis (PCA) and correlation analyses: The top three ligands with the highest binding affinities, namely ethyl 2-ethylhexanoate (102916), 3-buten-2-ol, 4-phenyl- (15172) and butanedioic acid (1110), were selected for molecular dynamics simulation (MDS). The protein–ligand complexes were subjected to a 300 ns simulation using the Schrödinger–Desmond module following previously reported methods [29]. Simulations were performed in an orthorhombic box using the TIP3P solvation model with a 10 Å buffer distance. System neutrality and osmotic balance were maintained by adding counter ions and 0.15 M NaCl. After equilibration, simulations were conducted at 310 K and 1.013 bar pressure [29,31]. Principal component analysis (PCA) and dynamic cross-correlation matrix (DCCM) analyses were subsequently performed to evaluate conformational dynamics and residue motion within the complexes [29].

ADMET properties prediction and evaluation of the Lipinski's rule of five: SwissADME and the pkCSM tools were employed to predict the ADMET properties of the bioactive compounds. These tools were used to generate molecular descriptions for the bioactive compounds. Subsequently, the predicted molecular descriptors were assessed to confirm compliance with Lipinski's rule of five.

RESULTS AND DISCUSSION

***In vitro* antibacterial activity:** Different fractions obtained from the aerial parts of *A. paniculata* against multi-drug-resistant (MDR) uropathogens are shown in Table-1. Among the tested fractions, the ethyl acetate fraction exhibited the highest antibacterial activity, producing inhibition zones ranging from 12-18 mm against all MDR uropathogens. In comparison, dichloromethane and methanol fractions showed inhibition zones of 8-16 mm and 10-14 mm, respectively. The stronger activity of the ethyl acetate fraction may be attributed to its intermediate polarity, which enables efficient extraction of both moderately polar and non-polar bioactive constituents [34-36]. Ethyl acetate is widely recognized as an effective extraction solvent due to its moderate polarity facilitates the separation of diverse phytochemicals with potential antimicrobial properties.

The minimum inhibitory concentration (MIC) results of the ethyl acetate fraction are shown in Table-2. A concentration of 6.25 mg/mL was sufficient to inhibit the growth of the tested MDR uropathogens, as evidenced by the absence of visible growth or colour change after 24 h incubation compared with the control. The minimum bactericidal concentration (MBC) results shown in Table-2 further demonstrated that 12.5 mg/mL of the ethyl acetate fraction exerted bactericidal activity against all tested organisms, since no bacterial growth

TABLE-1
ANTIBACTERIAL ACTIVITY DATA OF DIFFERENT FRACTIONS OF *A. paniculata* EXTRACT AGAINST SOME MULTIDRUG RESISTANT UROPATHPOGENS

MDR uropathogens	Negative control (DMSO)	Dichloromethane	Ethyl acetate	Methanol	Ciprofloxacin (positive control)
Klebsiella pneumoniae	0.00	10 mm	12 mm	11 mm	14 mm
Enterobacter cloacae	0.00	8 mm	16 mm	10 mm	18 mm
Staphylococcus ureilyticus	0.00	16 mm	18 mm	12 mm	21 mm
Escherichia coli	0.00	16 mm	12 mm	10 mm	20 mm
Bacillus cereus	0.00	10 mm	14 mm	14 mm	20 mm
Staphylococcus caprae	0.00	8 mm	16 mm	10 mm	18 mm

TABLE-2
MINIMUM INHIBITORY CONCENTRATION (MIC) AND MINIMUM BACTERICIDAL CONCENTRATION (MBC) (mg/mL) DATA OF ETHYL ACETATE FRACTION OF *A. paniculate*

Test organisms (MDR uropathogens)	Ethyl acetate fraction									
	100 mg/mL		50 mg/mL		25 mg/mL		12.5 mg/mL		6.25 mg/mL	
	MIC	MBC	MIC	MBC	MIC	MBC	MIC	MBC	MIC	MBC
Klebsiella pneumoniae	12 mm	–	12 mm	–	12 mm	–	10 mm	–	8 mm	+
Enterobacter cloacae	16 mm	–	16 mm	–	14 mm	–	12 mm	–	12 mm	+
Staphylococcus ureilyticus	18 mm	–	18 mm	–	14 mm	–	12 mm	–	8 mm	+
Escherichia coli	16 mm	–	16 mm	–	14 mm	–	10 mm	–	10 mm	+
Bacillus cereus	14 mm	–	14 mm	–	10 mm	–	10 mm	–	8 mm	+
Staphylococcus caprae	18 mm	–	16 mm	–	12 mm	–	10 mm	–	8 mm	+

– = No growth, + = Growth

TABLE-3
LIST OF BIOACTIVE COMPOUNDS ISOLATED FROM ETHYL ACETATE FRACTION OF *A. paniculate*

Name	m.f.	m.w.	Retention time	CAS number	Peak area (%)
Hexanoic acid	$C_6H_{12}O_2$	116	2.539	142-62-1	3.234
Hexanoic acid, 2-ethyl-, ethyl ester	$C_{10}H_{20}O_2$	172	6.716	2983-37-1	3.773
3-Buten-2-ol, 4-phenyl	$C_{10}H_{12}O$	148	6.911	17488-65-2	1.260
2-(1-Ethoxyethoxy) succinic acid, diethyl ester	$C_{12}H_{22}O_6$	262	11.437	Nil	2.504
Butanedioic acid, hydroxy-, diethyl ester, (±)	$C_8H_{14}O_5$	190	12.547	626-11-9	1.375
Undeca-3,4-diene-2,10-dione	$C_{11}H_{16}O_2$	180	13.559	Nil	1.001

was observed after subculturing onto nutrient-enriched media. These findings indicate that the bioactive compounds extracted into the ethyl acetate fraction possess significant antibacterial efficacy against MDR uropathogens. *In vitro* assays are important for evaluating the biological activity and therapeutic potential of plant-derived compounds under controlled laboratory conditions, providing preliminary evidence for their possible application in antimicrobial drug development.

Isolation of bioactive compounds from ethyl acetate fraction of *A. paniculata*: Since the ethyl acetate fraction exhibited the highest antibacterial activity during the *in vitro* assays, it was further subjected to phytochemical separation and identification of its bioactive constituents. TLC analysis revealed six distinct compounds with R_f values of 0.13, 0.24, 0.50, 0.63, 0.69 and 0.75 using chloroform:methanol (90:10) as the mobile phase. The separated spots were visualized under ultraviolet light. The same solvent system, which produced effective separation during TLC, was subsequently employed for column chromatography to isolate the bioactive constituents. The purified fractions obtained from column chromatography were further analysed using GC-MS for compound identification and structural elucidation. The GC-MS analysis identified six compounds, namely hexanoic acid, hexanoic acid 2-ethyl-ethyl ester, 3-buten-2-ol, 4-phenyl, 2-(1-ethoxyethoxy)-succinic acid diethyl ester, butanedioic acid hydroxy-diethyl ester (±) and undeca-3,4-diene-2,10-dione (Table-3). Mostly all the identified compounds are bioactive and contribute significantly antibacterial activity observed in the ethyl acetate fraction against multidrug-resistant uropathogens.

Molecular docking (MD): The docking analysis revealed differential interactions between the ligands and glucosamine-6-phosphate synthase (GlmS; PDB ID: 2VF5), as indicated by variations in binding energies (Table-4). The control ligand exhibited the strongest binding affinity with a docking score of -7.5 kcal/mol. Among the tested compounds, ligands 15172, 1110 and 102916 showed the highest binding affinities with docking scores of -5.4, -5.2 and -5.1 kcal/mol, respectively, suggesting relatively stable interactions within the active site of the target protein. Figs. 1 and 2 illustrate the two-dimensional and three-dimensional docking poses of the ligands, while Table-5 summarizes the detailed docking interactions and amino acid residues involved in binding.

The interaction analysis demonstrated that the control ligand formed interactions with 11 amino acid residues, namely Ser604, Thr352, Ser349, Ala602, Val399, Glu485, Gln348, Ala400, Ser401, Thr302 and Ser347. Ligand 1110 interacted with six residues, including Ser303, Thr302, Ser401, Lys603, Ser604 and Ser349. Ligand 15172 formed interactions

TABLE-4
BINDING AFFINITIES OF THE COMPLEXES

Ligands (PubChem CID)	Binding energy (kcal/mol)
2vf5_control	-7.5
Hexanoic acid (8892)	-4.4
Hexanoic acid, 2-ethyl-, ethyl ester (102916)	-5.1
3-Buten-2-ol, 4-phenyl (15172)	-5.4
2-(1-Ethoxyethoxy)succinic acid, diethyl ester (552076)	-4.8
Butanedioic acid, hydroxy-, diethyl ester, (±) (1110)	-5.2
Undeca-3,4-diene-2,10-dione (538547)	-4.9

TABLE-5
DETAILS OF DOCKING INTERACTIONS FOR THE LIGANDS

Ligand	Receptor	Interaction	Distance	Binding energy (kcal/mol)
2vf5_control				
N2 11	O VAL 399	H-donor	2.77	-10.0
N2 11	O ALA 602	H-donor	2.85	-10.6
O3 17	OE2 GLU 488	H-donor	2.66	-4.6
O4 21	OG SER 401	H-donor	2.94	-0.9
O1P 2	N GLN 348	H-acceptor	2.69	-7.7
O1P 2	N SER 349	H-acceptor	2.93	-8.0
O2P 3	NE2 GLN 348	H-acceptor	2.81	-7.3
O2P 3	N SER 349	H-acceptor	3.12	-1.4
O3P 4	OG SER 349	H-acceptor	2.51	-0.9
O3P 4	OG1 THR 352	H-acceptor	2.56	-2.8
O3P 4	CA SER 604	H-acceptor	3.16	-0.9
O3 17	N SER 401	H-acceptor	3.00	-2.2
O4 21	N THR 302	H-acceptor	2.92	-2.0
N2 11	OE2 GLU 488	Ionic	3.64	-1.4
2vf5_1110				
O2 9	OG SER 401	H-donor	2.71	-3.0
O4 8	OG SER 303	H-acceptor	2.79	-1.4
O3 12	N SER 349	H-acceptor	2.93	-3.8
O3 12	OG SER 349	H-acceptor	2.68	-1.3
2vf5 _15172				
O1 22	OG SER 347	H-donor	2.92	-0.7
O1 22	N GLN 348	H-acceptor	2.95	-2.3
O1 22	N SER 349	H-acceptor	2.89	-2.8
O1 22	OG SER 349	H-acceptor	2.78	-1.6
2vf5_102916				
O2 24	N GLN 348	H-acceptor	2.93	-2.0
O2 24	N SER 349	H-acceptor	2.90	-5.3
O2 24	OG SER 349	H-acceptor	2.76	-1.2

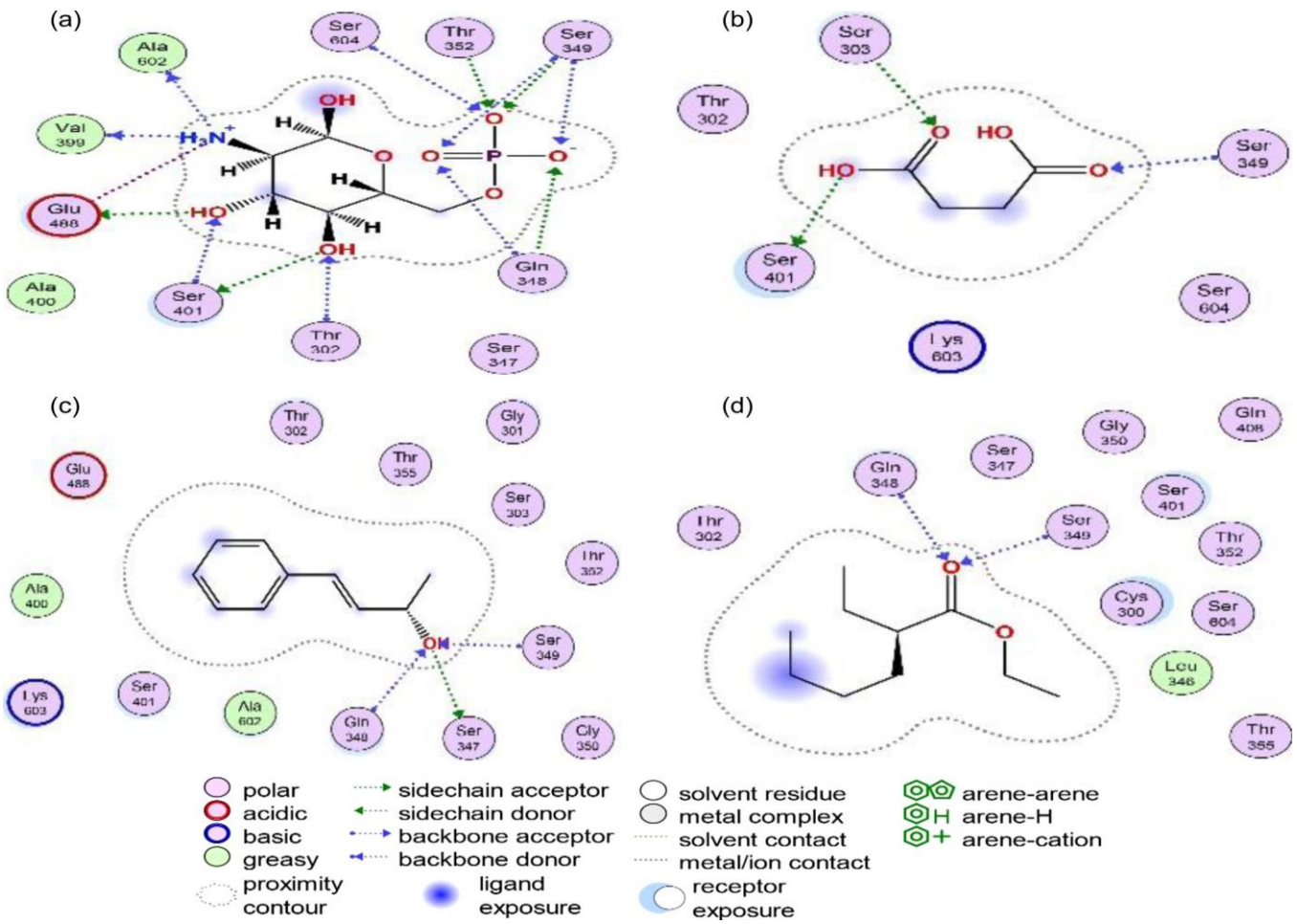

Fig. 1. Docking poses of the various complexes in 2D for the ligands and the control

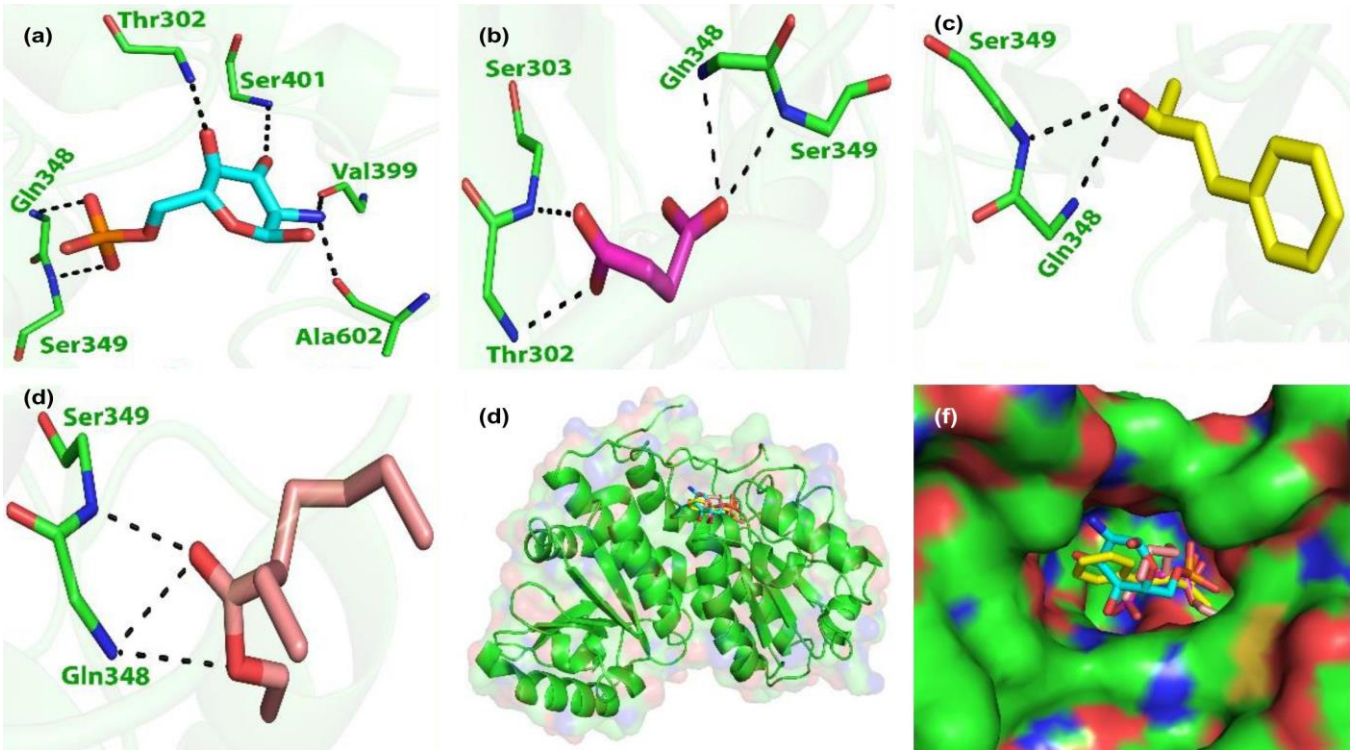

Fig. 2. Docking poses of the various complexes in 3D for the ligands (a-d) and the 3D protein complex-2VF5

with 14 amino acid residues, whereas ligand 102916 interacted with 12 residues. Significantly, Thr302, Ser349 and Ser401 were consistently involved in the binding of all three top-ranked ligands, indicating that these residues may play important roles in ligand stabilization within the active site. The stronger interaction profile observed for ligand 15172 may be associated with the presence of both a phenyl ring and allylic alcohol group, which could facilitate π-π stacking and hydrogen bonding interactions with active-site residues [37].

In present study, the moderate binding affinities of the identified phytocompounds suggest their potential to interact with GlmS through multiple mechanisms. Ligand 1110, containing a carboxyl functional group, may competitively inhibit substrate binding by mimicking fructose-6-phosphate, the natural substrate of the enzyme. In contrast, ligand 102916 may interact through hydrophobic forces within the glutamine-binding domain, thereby inducing conformational changes associated with allosteric inhibition [37-39]. Although the binding affinities of the phytocompounds were lower than that of the control ligand, the results indicate that the bioactive compounds identified from *A. paniculata* possess promising inhibitory potential against GlmS and may serve as lead molecules for further structural optimization and antimicrobial drug development.

Molecular dynamics (MD) simulation: The molecular dynamics (MD) simulation results for the top three ligands and the control complex over 300 ns are presented in Figs. 3-6. Root mean square deviation (RMSD) analysis (Fig. 3) demonstrated that protein backbone fluctuations were generally lower than ligand fluctuations throughout the simulation period. The control complex exhibited protein RMSD values ranging from 0.2-3.0 Å, whereas its ligand fluctuated between 0.8-6.4 Å. Ligand 1110 showed protein and ligand RMSD values of 0.8-3.6 Å and 1-8 Å, respectively, while ligand 15172 displayed protein RMSD values of 1.2-2.7 Å but substantially higher ligand fluctuations ranging from 10-80 Å. For ligand 102916, the RMSD values ranged from 1-3.75 Å for the protein and 1.6-5.6 Å for the ligand. Since RMSD values below 4 Å generally indicate stable complexes [40,41], the complexes formed by ligands 1110 and 102916 exhibited stability profiles most comparable to the control, suggesting relatively stable protein–ligand interactions [42-44].

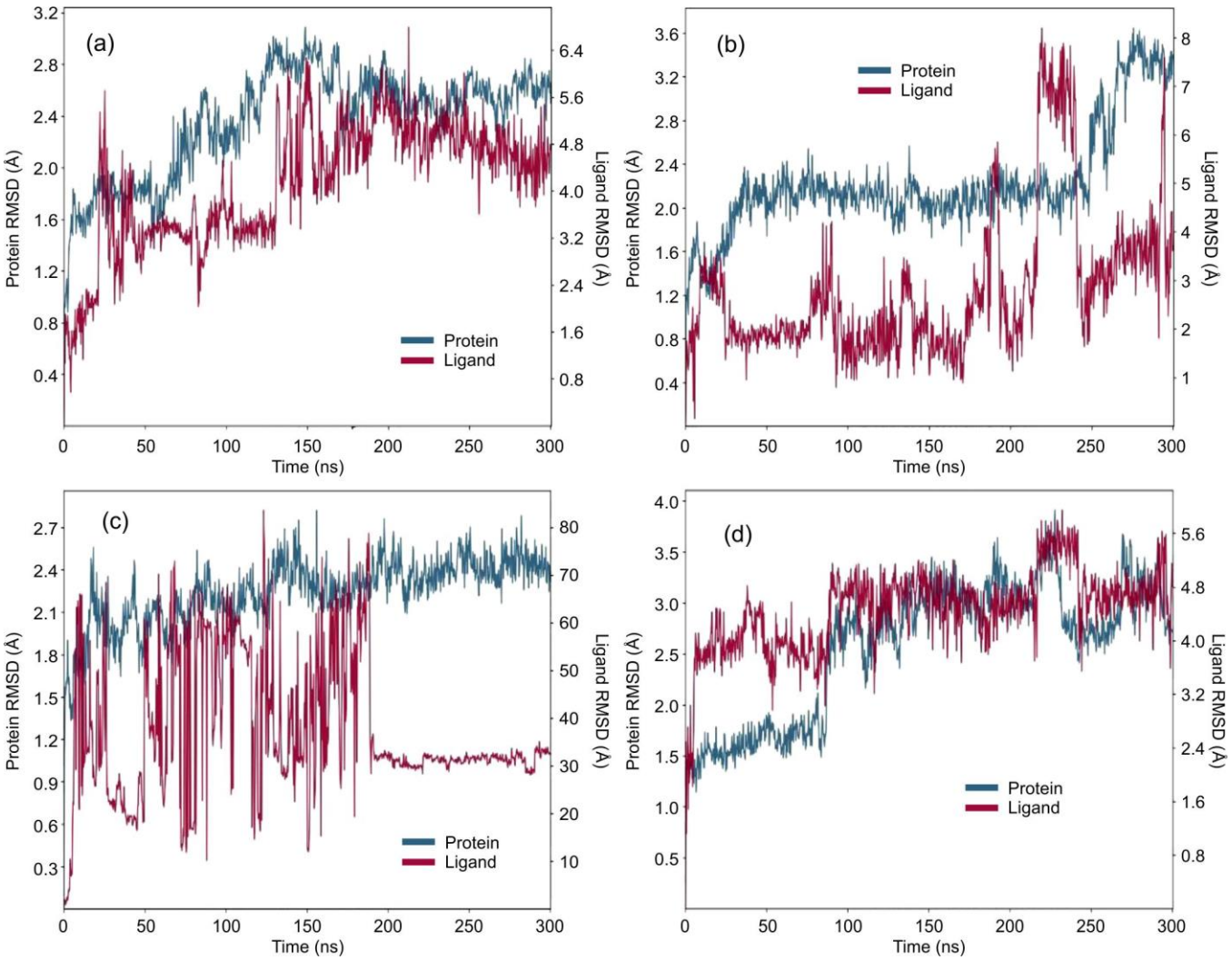

Fig. 3. RMSD trajectories of the protein–ligand complexes during the 300 ns molecular dynamics simulation of (a) control ligand, (b) butanedioic acid, (c) 3-buten-2-ol, 4-phenyl-, and (d) ethyl 2-ethylhexanoate

Root mean square fluctuation (RMSF) analysis (Fig. 4) revealed that most of the amino acid residues fluctuated within the range of 0.6-2.4 Å for both the control and ligand-bound complexes indicating stable residue mobility. However, high fluctuations above 2.4 Å were observed around residues 20, 260, 320 and 350, suggesting localized flexible regions that may influence complex stability. Interaction mapping (Fig. 5) showed variations in both the number and type of intermolecular interactions formed during the simulation. Hydrogen bonds represented the dominant interaction type, followed by water bridges, whereas ionic interactions were least abundant. Ligand 15172 formed the highest number of interacting residues and exhibited relatively stronger hydrophobic interactions compared with the other ligands, which may contribute to its favourable docking behaviour.

Fig. 6 illustrates the contact frequency between ligands and amino acid residues during the simulation. The control complex formed 25 contacts, whereas ligands 1110, 15172 and 102916 formed 20, 6 and 6 contacts, respectively. Persistent interactions were observed for residues Cys300, Thr302, Ser 303, Gln345, Ser349 and Thr352 in the control complex, while ligand 1110 maintained stable contacts with residues including Thr302, Ser303, Ser347, Gln348, Ser349 and Lys603. In contrast, ligands 15172 and 102916 did not maintain continuous residue contacts throughout the simulation, indicating comparatively weaker interaction persistence.

Additional analyses involving radius of gyration (rGyr), molecular surface area (MolSA), solvent accessible surface area (SASA) and polar surface area (PSA) were performed to evaluate molecular compactness and surface exposure [45-47]. The values obtained for the test ligands were generally comparable to those of the control complex, indicating similar structural compactness and folding behaviour. Ligand 15172 showed the highest MolSA values, reaching approximately 450 $Å^2$, whereas the PSA values of all test ligands remained lower than those of the control. Principal component analysis (PCA) further revealed that ligands 1110 and 102916 exhibited the highest conformational motion among the tested complexes, suggesting greater dynamic flexibility during the simulation period [29].

Ligand properties and PCA analyses: The ligand properties (RMSD, rGyr, MolSA, SASA and PSA) were also evaluated and the results are shown in Fig. 7. The RMSD values for the control and ligands 1110, 15172 and 102916, the values ranged from 0.25-1.5, 0.25-0.6, 0.125-1.0 and 0.6-0.8 Å, respectively. For rGyr, the values ranged from 2.85 to

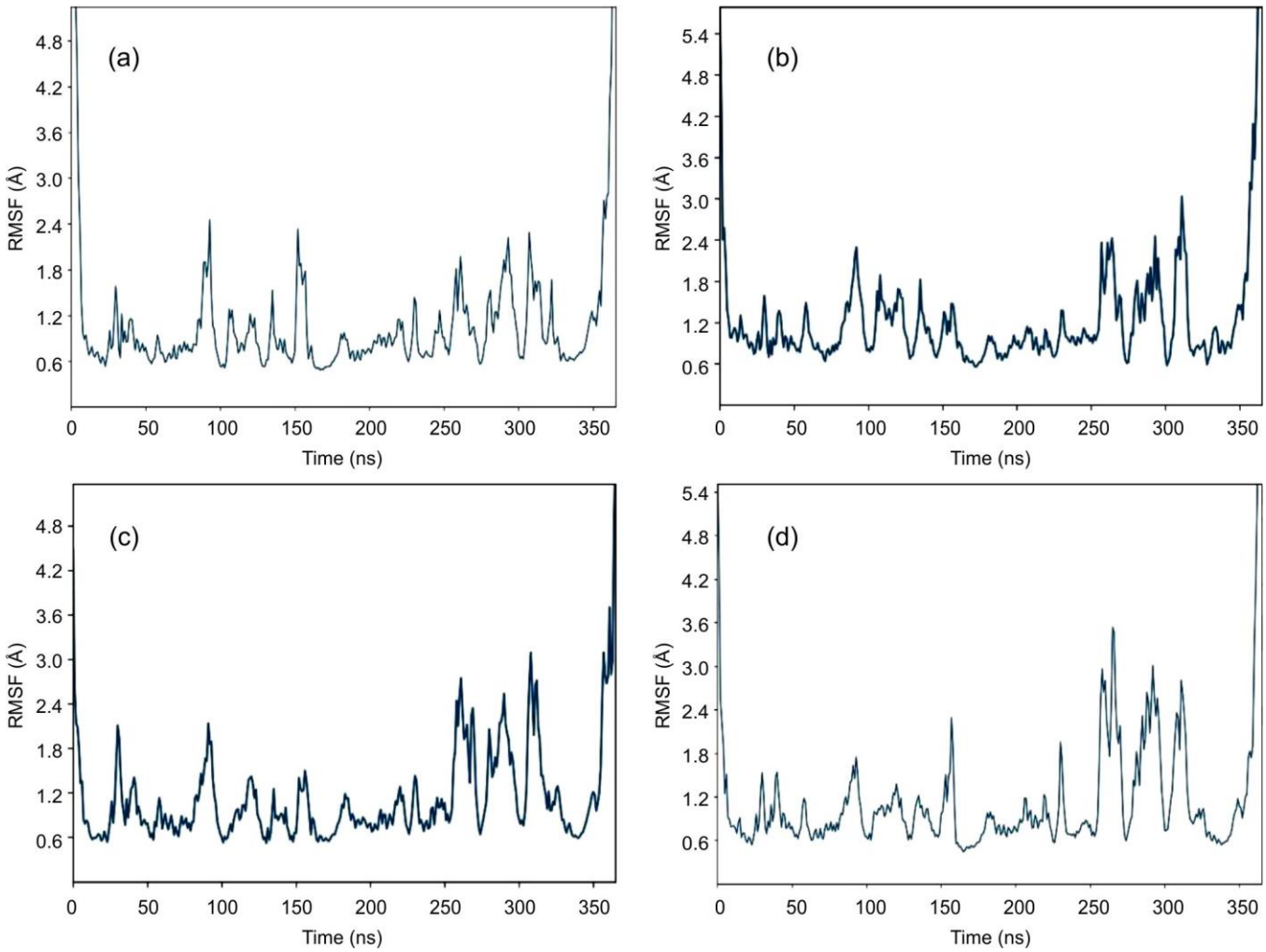

Fig. 4. RMSF trajectories of the protein–ligand complexes during the 300 ns molecular dynamics simulation of (a) control ligand, (b) butanedioic acid, (c) 3-buten-2-ol, 4-phenyl- and (d) ethyl 2-ethylhexanoate

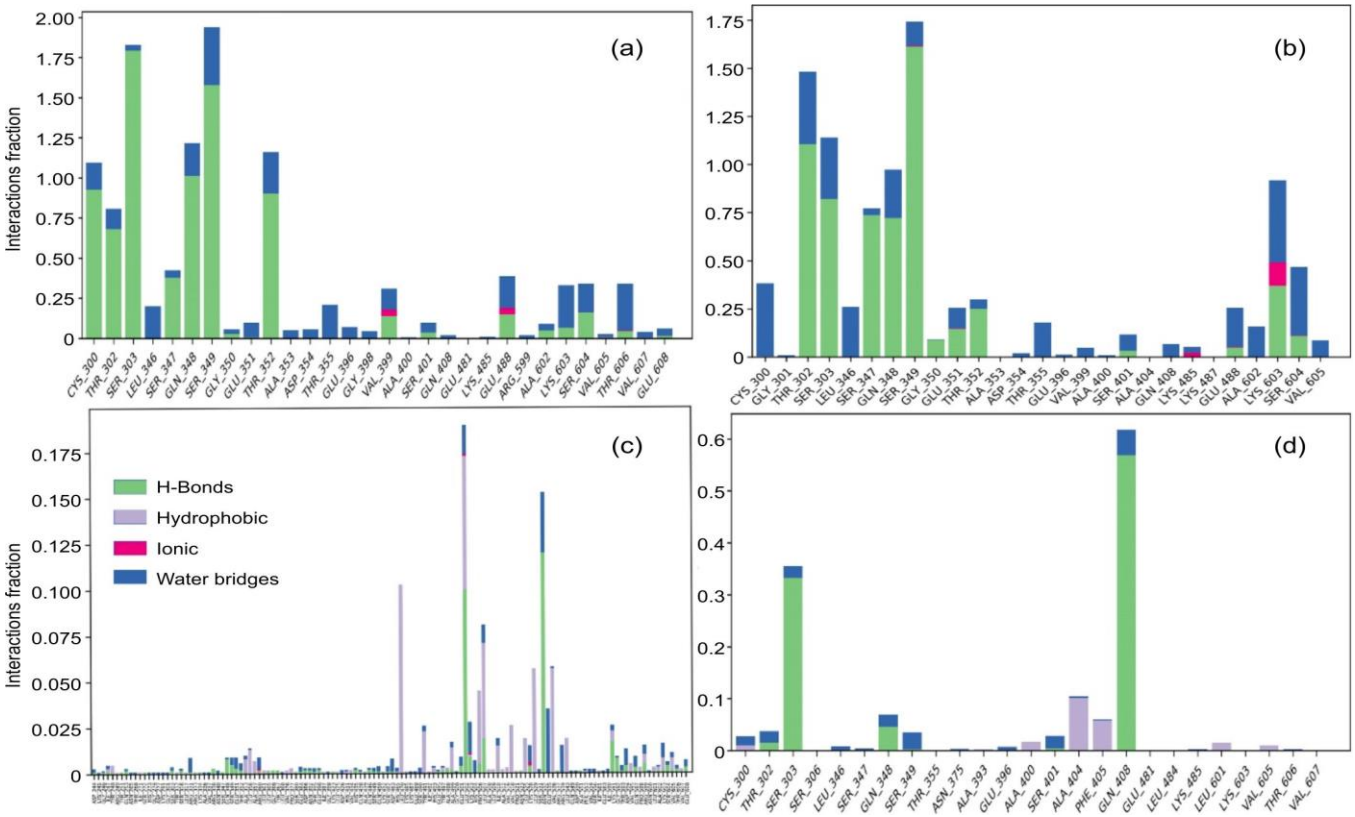

Fig. 5. Interaction profiles of amino acid residues and their corresponding bonding interactions in the protein–ligand complexes of (a) control ligand, (b) butanedioic acid, (c) 3-buten-2-ol, 4-phenyl-, and (d) ethyl 2-ethylhexanoate

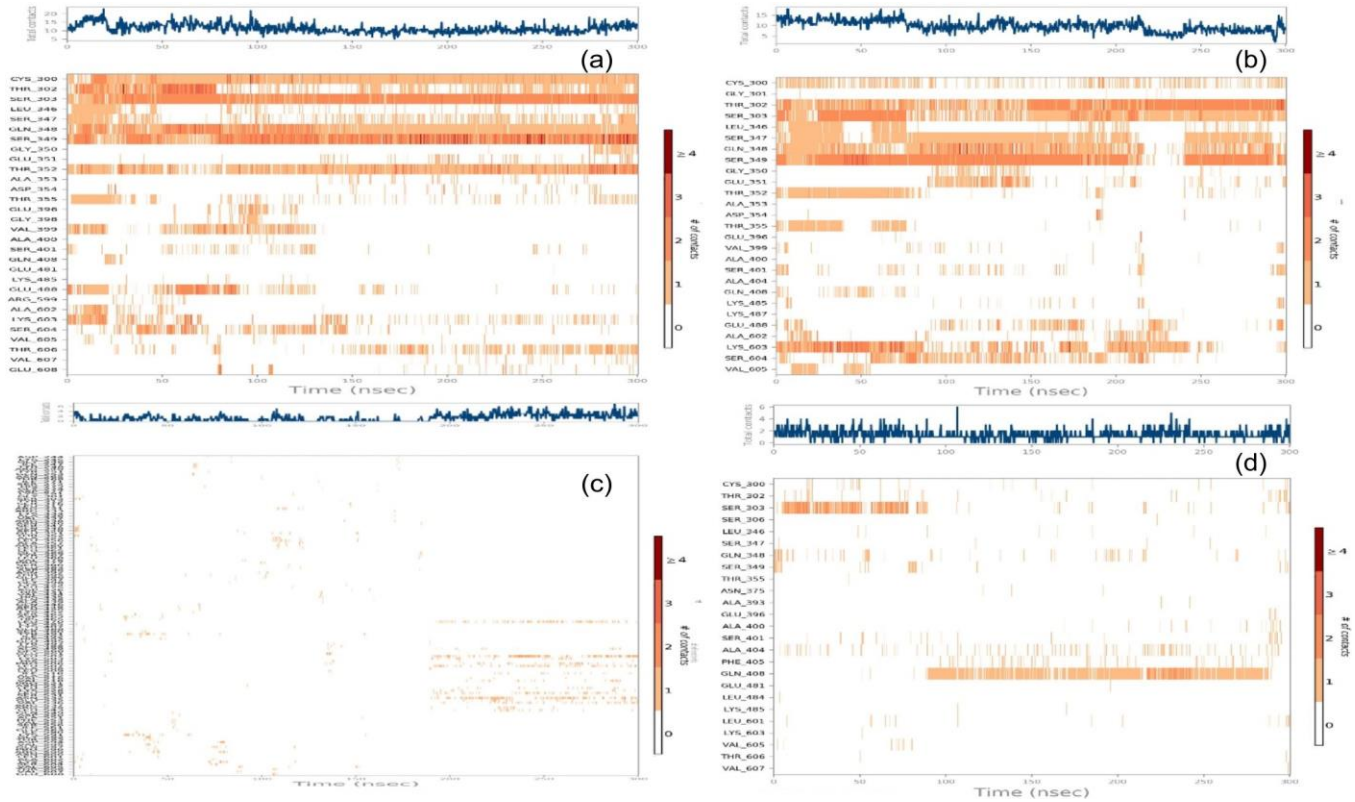

Fig. 6. Time-dependent contact frequency and interaction persistence of amino acid residues during the 300 ns molecular dynamics simulation of glucosamine-6-phosphate synthase (PDB ID: 2VF5) complexes with (a) control ligand, (b) butanedioic acid, (c) 3-buten-2-ol, 4-phenyl-, and (d) ethyl 2-ethylhexanoate

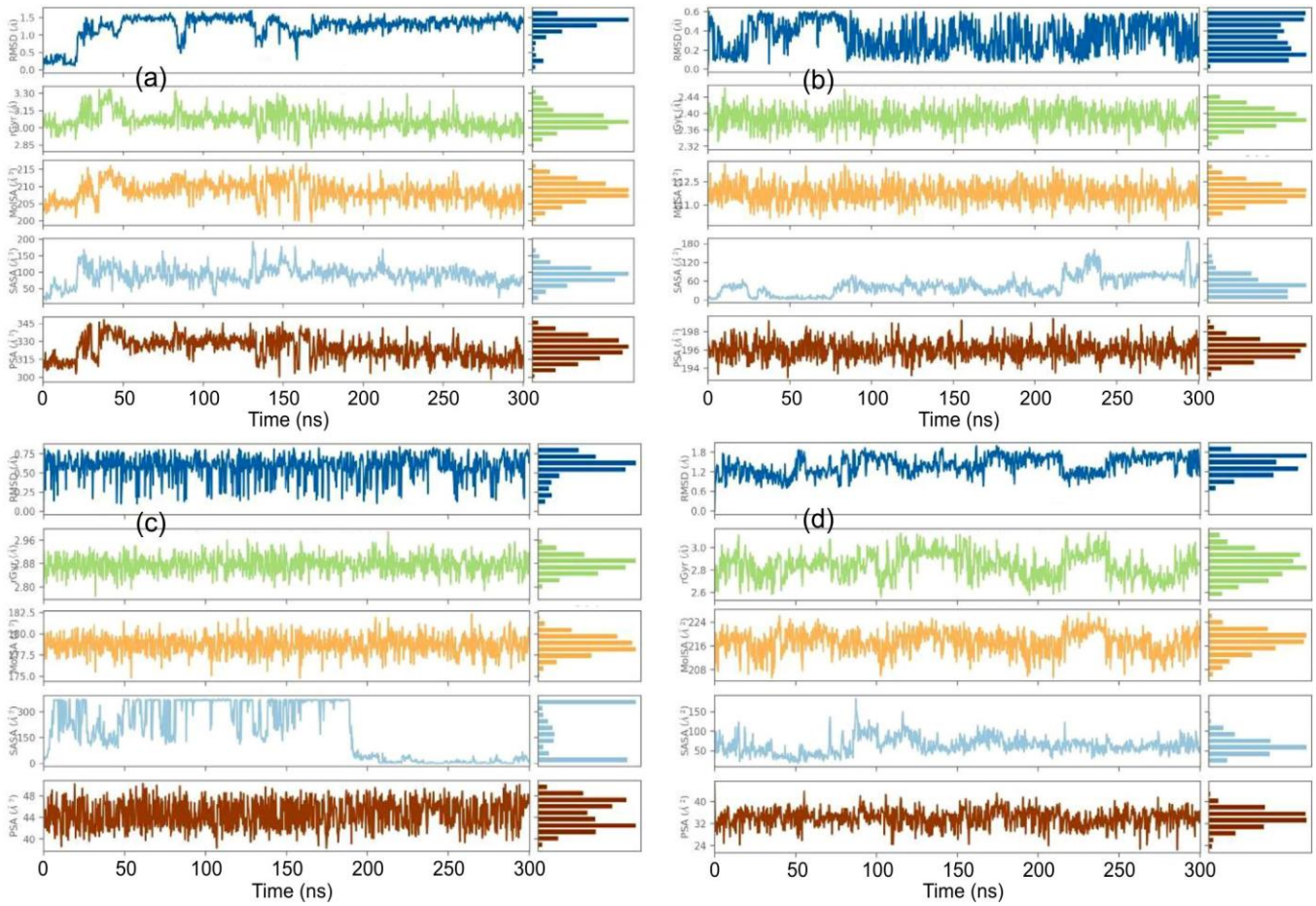

Fig. 7. RMSD, rGyr, MolSA, SASA and PSA plots of (a) control ligand, (b) butanedioic acid, (c) 3-buten-2-ol, 4-phenyl-, and (d) ethyl 2-ethylhexanoate

3.30, 2.32 to 244, 2.80 to 2.96 and 2.6 to 3.0 Å. The MolSA values of the ligands ranged from 200 to 215, 0 to 180, 175 to 182.5 and 208 to 204 Å^2. Their SASA values ranged from 25-100, 0-180, 0-450 and 25-175 Å^2. The PSA values of the ligands ranged from 300-345, 194-198, 40-52 and 24-48 Å^2. The results of the PCA for the various test ligands and the control is shown in Fig. 8. For all the test ligands and the control complex, the principal components PC1, PC2 and PC3 were plotted against each other in the PCA analyses. The results showed that PC1 contributed the highest proportion of conformational motion in all complexes. Combined contributions of PC1-PC3 accounted for 60.34%, 45.63%, 61.36% and 56.86% of the total variance for the control, ligands 1110, 15172 and 102916, respectively, indicating that these principal components captured the major dynamic motions of the protein–ligand complexes during the simulation period.

ADMET properties prediction and evaluation of the Lipinki's rule of five of the bioactive compounds: The molecular descriptors and ADMET properties of the identified bioactive compounds and the standard drug are shown in Tables 6 and 7. The molecular weights of the compounds ranged from 116.16-262.30 g/mol, indicating that the compounds are relatively small molecules with favourable characteristics for drug development. According to Lipinski's rule of five, compounds with molecular weights below 500 g/mol generally possess good oral bioavailability; none of the identified compounds violated this rule, suggesting promising drug-like potential. The high absorption values recorded for the bioactive compounds (93.44-100%) further indicate favourable oral absorption and permeability characteristics.

All the compounds exhibited negative water solubility values indicating moderate aqueous solubility, a property important for drug absorption and distribution [34]. Skin permeability analysis showed that some compounds, including the control, possessed permeability values above -2.5 cm/s, while others ranged between -1.8 and -2.1 cm/s, suggesting moderate transdermal permeability suitable for potential topical formulations [35,42,48,49]. The volume of distribution (VD) values indicated that several compounds may distribute effectively into body tissues, with some ligands exhibiting higher VD values than the control. Since higher VD values are associated with broader tissue distribution [41,50], these compounds may possess improved systemic distribution characteristics.

Blood–brain barrier (BBB) analysis revealed poor brain distribution for all compounds, whereas central nervous system (CNS) permeability values (Log Ps > -2) suggested limited but possible CNS penetration [43,51]. Cytochrome P450 profiling demonstrated that none of the bioactive compounds acted as inhibitors or substrates of major CYP isoenzymes including CYP3A4, CYP2D6, CYP2C9, CYP1A2 and CYP2C19, indicating reduced likelihood of adverse drug–drug interactions and metabolic complications [52]. Toxicity profiling further

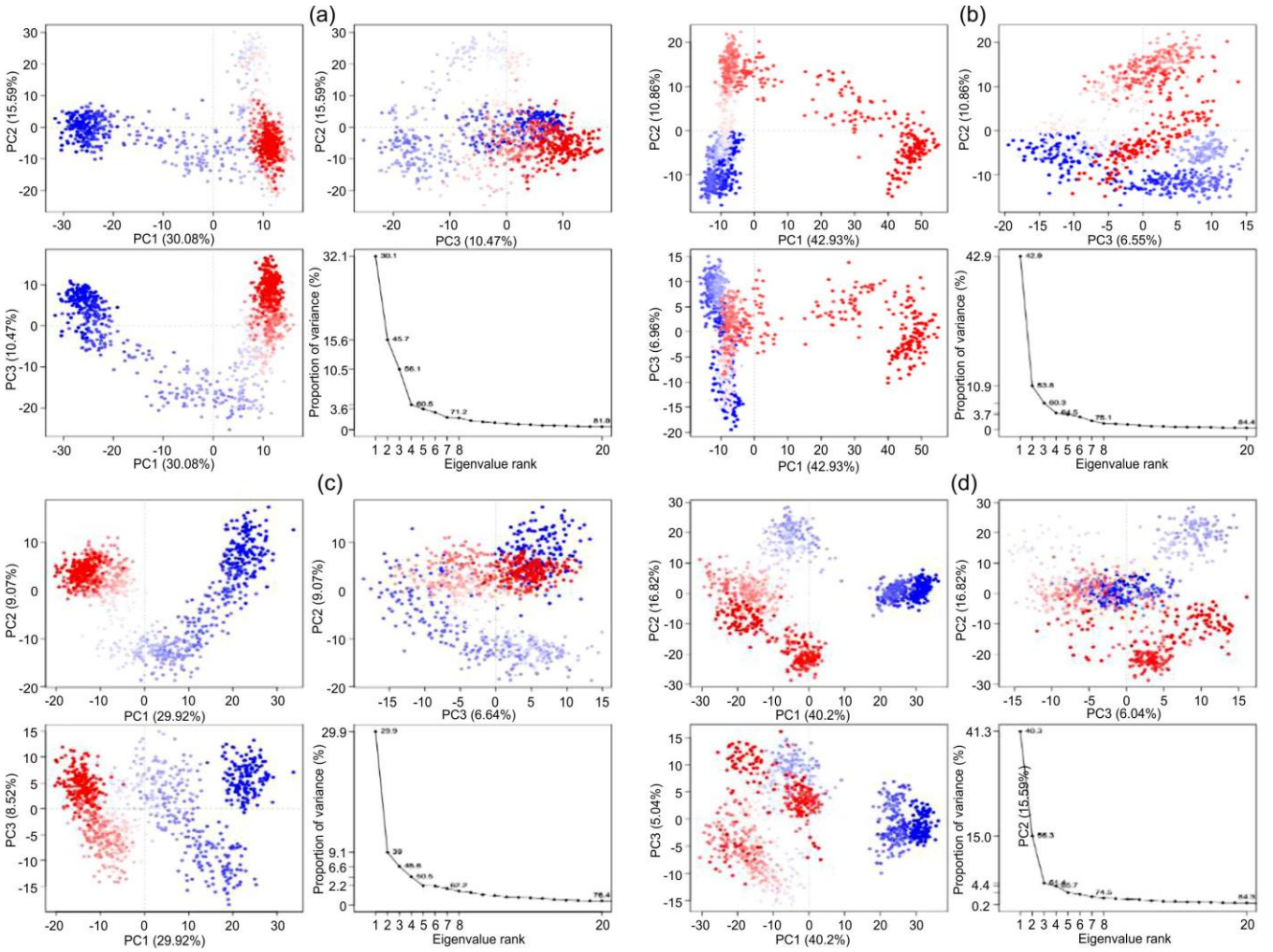

Fig. 8. PCA and eigenvalue rank plots of (a) control ligand, (b) butanedioic acid, (c) 3-buten-2-ol, 4-phenyl-, and (d) ethyl 2-ethylhexanoate

TABLE-6
MOLECULAR DESCRIPTORS OF THE VARIOUS BIOACTIVE COMPOUNDS (LIGAND) AND A STANDARD DRUG (CONTROL)

Properties	Hexanoic acid, 2-ethyl-, ethyl ester	3-Buten-2-ol, 4-phenyl	Butanedioic acid, hydroxy-, diethy ester, (±)	Control (ciprofloxacin)
Formula	$C_{10}H_{20}O_2$	$C_{10}H_{12}O$	$C_8H_{14}O_5$	$C_{17}H_{18}FN_3O_3$
Molecular weight	172.26g/mol	148.20g/mol	190.19g/mol	331.34g/mol
Number of heavy atoms	12	11	13	24
Number of aromatic heavy atoms	0	6	0	10
Fraction Csp^3	0.90	0.20	0.75	0.41
Number of rotatable bonds	7	2	7	3
Number of hydrogen-bonds acceptors	2	1	5	5
Number of hydrogen-bonds donor	0	1	1	2
Molar refractivity	51.47	47.31	44.30	95.25
TPSA (topological polar surface area)	26.30 Å^2	20.23 Å^2	72.83 Å^2	74.57 Å^2

showed that all compounds were AMES negative, suggesting absence of mutagenic potential and lower carcinogenic risk [51]. In addition, none of the bioactive compounds exhibited hepatotoxicity, whereas the control drug ciprofloxacin showed predicted hepatotoxic effects, consistent with previous reports associating ciprofloxacin with liver injury, hepatitis and high hepatic enzyme levels [38,51]. These findings indicate that the identified bioactive compounds possess favourable pharmacokinetic, safety and drug-likeness properties, supporting their potential as promising antimicrobial candidates against multidrug resistant uropathogens.

Conclusion

The present study demonstrated that the ethyl acetate fraction of *Andrographis paniculata* exhibited significant antibacterial activity against multidrug-resistant uropathogens, with inhibition zones ranging from 12-18 mm, MIC of 6.25 mg/mL and MBC of 12.5 mg/mL. GC-MS analysis identified

TABLE-7
ADMET PROPERTIES OF THE BIOACTIVE COMPOUNDS

ADMET/Unit	Bioactive compounds (Ligands)			
	Hexanoic acid, 2-ethyl-, ethyl ester	3-Buten-2-ol, 4-phenyl	Butanedioic acid, hydroxy-, diethy ester, (±)	Control (ciprofloxacin)
Absorption				
Water solubility (Log mol/L)	-2.803	-1.732	0.115	-2.897
$CaCO_2$ permeability (log papp in 10^{-6} cm/s)	1.607	1.405	0.852	0.492
Intestinal absorption (human) (% absorbed)	94.955	94.4	92.163	96.466
Skin permeability (Log kp)	-1.814	-2.001	-2.873	-2.734
P-Glycoprotein substrate (yes/no)	No	No	No	Yes
P-Glycoprotein 1 inhibitor (yes/no)	No	No	No	No
P-Glycoprotein 11 inhibitor (yes/no)	No	No	No	No
Distribution				
VDss (human) (Log L/kg)	0.078	0.123	-0.193	-0.17
Fraction unbound (human) (Fu)	0.462	0.342	0.766	0.648
BBB permeability (Log BB)	0.586	0.306	-0.435	-0.587
CNS permeability (Log Ps)	-2.321	-1.292	-3.027	-2.999
Metabolism				
CYP2D6 substrate (yes/no)	No	No	No	No
CYP3A4 substrate (yes/no)	No	No	No	No
CYP1A2 substrate (yes/no)	No	No	No	No
CYP2C19 substrate (yes/no)	No	No	No	No
CYP2C9 substrate (yes/no)	No	No	No	No
CYP2D6 substrate (yes/no)	No	No	No	No
CYP3A4 substrate (yes/no)	No	No	No	No
Excretion				
Total clearance (Log mL/min/kg)	1.671	0.284	1.022	0.633
Renal OCT2 substrate (yes/no)	No	No	No	No
Toxicity				
AMES toxicity (yes/no)	No	No	No	No
Maximum tolerated dose (human) (Log mg/kg/day)	0.599	0.584	0.993	0.924
LERG 1 inhibitor (yes/no)	No	No	No	No
LERG 11 inhibitor (yes/no)	No	No	No	No
Oral rat acute toxicity (LD_{50}) (mol/kg)	1.834	2.153	1.93	2.891
Oral rat chronic toxicity (LOAEL) (Log mg/kg-bw/day)	2.341	1.964	1.195	1.036
Hepatoxicity (yes/no)	No	No	No	Yes
Skin sensation (yes/no)	Yes	Yes	No	No
T. *pyriformis* toxicity (Log µg/L)	0.683	0.173	-0.411	0.286
Mininow toxicity (Log mm)	0.787	1.042	2.238	1.194

several bioactive compounds, among which hexanoic acid 2-ethyl-ethyl ester, 3-buten-2-ol, 4-phenyl and butanedioic acid hydroxy-diethyl ester (±) showed promising interactions with glucosamine-6-phosphate synthase (GlmS), a key enzyme involved in bacterial peptidoglycan biosynthesis. Molecular docking analysis revealed favourable binding affinities, with 3-buten-2-ol, 4-phenyl exhibiting the strongest interaction among the phytocompounds. Important amino acid residues such as Thr302, Ser349 and Ser401 were consistently involved in ligand binding, indicating their role in active-site stabilisation. MD simulations confirmed the stability of the ligand–protein complexes, particularly for ligands 1110 and 102916, which showed RMSD and RMSF profiles comparable to the control complex during the 300 ns simulation period. The hydrogen bonding and hydrophobic interactions contributed significantly to complex stability. ADMET analysis indicated favourable pharmacokinetic and safety properties, including high oral absorption, acceptable tissue distribution, absence of CYP inhibition and non-hepatotoxic behaviour. None of the compounds violated Lipinski's rule of five, suggesting promising drug-like characteristics. These findings indicate that bioactive compounds isolated from *A. paniculata* possess considerable potential as lead molecules for the development of safer antimicrobial agents against multidrug-resistant uropathogens associated with urinary tract infections (UTI).

CONFLICT OF INTEREST

The authors declare that there is no conflict of interests regarding the publication of this article.

DECLARATION OF AI-ASSISTED TECHNOLOGIES

During the preparation of this manuscript, the authors used an AI-assisted tool(s) to improve the language. The authors reviewed and edited the content and take full responsibility for the published work.

REFERENCES

1. A.L. Flores-Mireles, J.N. Walker, M. Caparon and S.J. Hultgren, *Nat. Rev. Microbiol.*, **13**, 269 (2015); https://doi.org/10.1038/nrmicro3432
2. B. Foxman, *Nat. Rev. Urol.*, **7**, 653 (2010); https://doi.org/10.1038/nrurol.2010.190
3. K. Gupta, T.M. Hooton, K.G. Naber, B. Wullt, R. Colgan, L.G. Miller and D.E. Soper, *Clin. Infect. Dis.*, **52**, e103 (2011); https://doi.org/10.1093/cid/ciq257
4. R.G. Jepson, G. Williams and J.C. Craig, *Cochrane Database Syst. Rev.*, **10**, CD001321 (2012); https://doi.org/10.1002/14651858.CD001321.pub5
5. K.A. Kline and D.M.E. Bowdish, *Curr. Opin. Microbiol.*, **29**, 63 (2016); https://doi.org/10.1016/j.mib.2015.11.003
6. R. Raz and W.E. Stamm, *N. Engl. J. Med.*, **329**, 753 (1993); https://doi.org/10.1056/NEJM199309093291102
7. W.E. Stamm and S.R. Norrby, *J. Infect. Dis.*, **183(S1)**, S1 (2001); https://doi.org/10.1086/318850
8. P.A. Tambyah and D.G. Maki, *Arch. Intern. Med.*, **160**, 678 (2000); https://doi.org/10.1001/archinte.160.5.678
9. C.L. Ventola, *P&T*, **40**, 277 (2015); https://doi.org/10.1097/NMC.0000000000000166
10. B. Kot, *Pol. J. Microbiol.*, **68**, 403 (2019); https://doi.org/10.33073/pjm-2019-048
11. D.D. Caceres, J.L. Hancke, R.A. Burgos, F. Sandberg and G.K. Wikman, *Phytomedicine*, **4**, 101 (1997); https://doi.org/10.1016/S0944-7113(97)80051-7
12. S. Boro, M. Chirania, D. Boro, B. Bharadwaj, M. Baruah and M. Bhattacharjee, *Univ. Med.*, **45**, 113 (2026); https://doi.org/10.18051/UnivMed.2026.v45.113-124
13. T. Jayakumar, C.Y. Hsieh, J.J. Lee and J.R. Sheu, *Evid. Based Complement. Alternat. Med.*, **2013**, 846740 (2013); https://doi.org/10.1155/2013/846740
14. U.O. Edet, E.N. Mbim, E. Ezeani, O.U. Henshaw, O.R. Ibor, I.U. Bassey and A.F. Nneoyi-Egbe, *BMC Complement. Med. Ther.*, **23**, 39 (2023); https://doi.org/10.1186/s12906-023-03841-z
15. S. R. Panda, A. Meher, G. Prusty, S. Behera and B.R. Prasad, *Discov. Plants*, **2**, 21 (2025); https://doi.org/10.1007/s44372-025-00097-4
16. S. Fathima, P.C. Jambiga, R. Thumma, S. Ahmadi, B.S. Mohammed, S. Askani, P. Sutramay, S.B. Dharavath and S. Taduri, *J. Phytopharmacol.*, **12**, 305 (2023); https://doi.org/10.31254/phyto.2023.12505
17. P.K. Singha, S. Roy and S. Dey, *Fitoterapia*, **74**, 692 (2003); https://doi.org/10.1016/S0367-326X(03)00159-X
18. S. Hossain, Z. Urbi, H. Karuniawati, R.B. Mohiuddin, A. Moh Qrimida, A.M.M. Allzrag, L.C. Ming, E. Pagano and R. Capasso, *Life*, **11**, 348 (2021); https://doi.org/10.3390/life11040348
19. Y.C. Shen, C.F. Chen and W.F. Chiou, *Br. J. Pharmacol.*, **135**, 399 (2002); https://doi.org/10.1038/sj.bjp.0704493
20. P.K. Singha, S. Roy and S. Dey, *Fitoterapia*, **74**, 692 (2003); https://doi.org/10.1016/S0367-326X(03)00159-X
21. U.O. Edet, U.M. Ekanemesang, C.A. Etok, G.M. Ikon and M.K. Noble, *Asian J. Med. Health.*, **1**, 1 (2016); https://doi.org/10.9734/AJMAH/2016/29460
22. K. Sheeja and G. Kuttan, *Integr. Cancer Ther.*, **6**, 389 (2007); https://doi.org/10.1177/1534735406298975
23. G. Sliwoski, S. Kothiwale, J. Meiler and E.W. Lowe, *Pharmacol. Rev.*, **66**, 334 (2014); https://doi.org/10.1124/pr.112.007336
24. J. Stefaniak, M.G. Nowak, M. Wojciechowski, S. Milewski and A.S. Skwarecki, *J. Enzyme Inhib. Med. Chem.*, **37**, 1928 (2022); https://doi.org/10.1080/14756366.2022.2096018
25. K. Banerjee, U. Gupta, S. Gupta, G. Wadhwa, R. Gabrani, S.K. Sharma and C.K. Jain, *Bioinformation*, **7**, 285 (2011); https://doi.org/10.6026/007/97320630007285
26. A. Sofowora, Medicinal Plants and Traditional Medicine in Africa, Spectrum Books Ltd., Ibadan, Nigeria, pp. 191-289 (1993).
27. F.O. Nwaokorie, U.O. Edet, A.P. Joseph, K. Phylis and O. Folasade, *Sci. Afr.*, **19**, e01445 (2023); https://doi.org/10.1016/j.sciaf.2022.e01445
28. S. Mouilleron, M.-A. Badet-Denisot and B. Golinelli-Pimpaneau, *J. Mol. Biol.*, **377**, 1174 (2008); https://doi.org/10.1016/j.jmb.2008.01.077
29. B. Kubra, S.L. Badshah, S. Faisal, M. Sharaf, A.H. Emwas, M. Jaremko and M. Abdalla, *J. Biomol. Struct. Dyn.*, **41**, 9103 (2023); https://doi.org/10.1080/07391102.2022.2140201
30. F. Nwaokorie, M. Abdalla, U.O. Edet, A.M. Abdalla, E.A. Okpo, A. Shami and S.C. Alaribe, *J. Mol. Struct.*, **1316**, 138733 (2024); https://doi.org/10.1016/j.molstruc.2024.138733
31. W. Huang, S. Lu, Z. Huang, X. Liu, L. Mou, Y. Luo, Y. Zhao, Y. Liu, Z. Chen, T. Hou and J. Zhang, *Bioinformatics*, **29**, 2357 (2013); https://doi.org/10.1093/bioinformatics/btt399
32. W.L. DeLano, *Drug Discov. Today*, **10**, 213 (2005); https://doi.org/10.1016/S1359-6446(04)03363-X
33. L. Guan, H. Zhang, Y. Zhong and Y. Liu, *MedChemComm*, **10**, 148 (2018); https://doi.org/10.1039/C8MD00472B
34. M. Miar, F. Mirjalili, H. Esfandiari, Z. Zare and M. Pourayoubi, *J. Chem. Res.*, **45**, 147 (2021); https://doi.org/10.1177/1747519820932091
35. Z.D.C.D. Merces, N.M. Salvadori, S.M. Evangelista, T.B. Cochlar, V.J. Strasburg, V.L. Da Silva and V.R.D. Oliveira, *Foods*, **13**, 3217 (2024); https://doi.org/10.3390/foods13203217
36. G.M. Cragg and D.J. Newman, *General Subjects*, **1830**, 3670 (2013); https://doi.org/10.1016/j.bbagen.2013.02.008
37. R. Vaidyanathan, S.M. Sreedevi, K. Ravichandran, S.M. Vinod, Y.H. Krishnan, L.K. Babu, P.S. Parthiban, L. Basker, T. Perumal, V. Rajaraman, G. Arumugam, K. Rajendran and V. Mahalingam, *JCIS Open*, **12**, 100096 (2023); https://doi.org/10.1016/j.jciso.2023.100096
38. X. Lv, W. Li, M. Zhang, R. Wang and J. Chang, *J. Mol. Recogn.*, **37**, e3075 (2024); https://doi.org/10.1002/jmr.3075
39. E.L. Kechi, B.E. Inah, O.C. Godfrey, U.O. Edet, O.J. Ikenyirimba, E.E. Antai, and H. Louis, *J. Mol. Struct.*, **1292**, 136048 (2023); https://doi.org/10.1016/j.molstruc.2023.136048
40. C. Savojardo, M. Manfredi, P.L. Martelli and R. Casadio, *Front. Mol. Biosci.*, **7**, 626363 (2021); https://doi.org/10.3389/fmolb.2020.626363
41. B.G. Katzung, T.W. Vanderah and A.J. Trevor, Basic and Clinical Pharmacology, McGraw Hill, edn 15 (2021).
42. G.P. Kamatou, I. Vermaak and A.M. Viljoen, *Molecules*, **17**, 6953 (2012); https://doi.org/10.3390/molecules17066953
43. M. Abdalla, W.A. Eltayb, A.A. El-Arabey, K. Singh and X. Jiang, *Comput. Biol. Med.*, **141**, 105025 (2022); https://doi.org/10.1016/j.compbiomed.2021.105025
44. S. Rampogu, G. Lee, J.S. Park, K.W. Lee and M.O. Kim, *Int. J. Mol. Sci.*, **23**, 1771 (2022); https://doi.org/10.3390/ijms23031771
45. M. Arnittali, A.N. Rissanou and V. Harmandaris, *Procedia Comput. Sci.*, **156**, 69 (2019); https://doi.org/10.1016/j.procs.2019.08.181
46. W.M. Pardridge, *NeuroRx*, **2**, 3 (2005); https://doi.org/10.1602/neurorx.2.1.3
47. D.E. Pires, T.L. Blundell and D.B. Ascher, *J. Med. Chem.*, **58**, 4066 (2015); https://doi.org/10.1021/acs.jmedchem.5b00104
48. S. Sangthong, P. Chaiwut, P. Pintathong, B. Suwannawong, M. Srisayam, T. Theansungnoen, K. Chandarajoti, H. Arabnozari, S.D. Sarker and L. Nahar, *Sci. Rep.*, **15**, 37263 (2025); https://doi.org/10.1038/s41598-025-21278-x
49. C.L. Linster and E. Van Schaftingen, *Annu. Rev. Biochem.*, **89**, 653 (2020);
50. U.M. Zanger and M. Schwab, *Pharmacol. Ther.*, **138**, 103 (2013); https://doi.org/10.1016/j.pharmthera.2012.12.007
51. M.A. Contreras, J. Luna, G. Mulero and J. Andreu, *Eur. J. Clin. Microbiol. Infect. Dis.*, **20**, 434 (2001); https://doi.org/10.1007/s10096-001-8144-2
52. I.E. Andy, E.A. Okpo and I.E. Ekon, *Afr. J. Biomed. Res.*, **25**, 403 (2022).